Journal of Engineering and Sustainable Development
Vol. 21, No. 02, March 2017
ISSN 2520-0917
www.jeasd.org

# EXPERIMENTAL AND NUMERICAL SIMULATION OF FLOW OVER BROAD CRESTED WEIR AND STEPPED WEIR USING DIFFERENT TURBULENCE MODELS

*Dr. Shaymaa A. M. Al-Hashimi[1], Dr. Huda M. Madhloom[2], Thameen Nazar Nahi[3]

1) Assist Prof. , Civil Engineering Department, Al-Mustansiriayah University, Baghdad, Iraq.
2) Lecture, Civil Engineering Department, Al-Mustansiriayah University, Baghdad, Iraq.
3) M.Sc. Student, Civil Engineering Department, Al-Mustansiriayah University, Baghdad, Iraq.

**Abstract:** A broad-crested weir has been considered the most hydraulic structures which was used in open channels for flow measurement and to control the water surface levels due to its simplicity. Both experimental and numerical models were conducted on a broad crested weir and stepped weir with a rounded corner. In this study, FLUENT software as a type of Computational Fluid Dynamics (CFD) model, represented as a numerical model in order to simulate flow over weirs that govern by Reynold averaged Navier Stoke equation and their results were compared with experimental results. The structured mesh with high concentration near the wall regions was employed in the numerical model. The volume of fluid (VOF) method with four turbulence models of Standard k–ε, RNG k–ε, Realizable k–ε and Standard k–ω are applied to estimate the free surface profile. The result showed that the flow over weirs is turbulent and the characteristics of free surface were complex and often difficult to be predicted. Also, the comparison of water surface profile between experimental value and numerical results obtained from the turbulent models showed that the standard k–ε model has the best similarity and standard k–ω model has the minimum similarity with experimental value.

**Keywords**: *Broad Crested Weir, Stepped Weir, Numerical CFD Model, FLUENT, VOF, Turbulent Models.*

**الخلاصة:** يعتبر السد واسع القمة من اكثر المنشاءات الهيدروليكية التي استخدمت في القنوات المفتوحة لقياس الجريان والتحكم في مستويات المياه السطحية نظراً لبساطته. كلا النماذج العددية والتجريبية أجريت على السد واسع القمة والسد المدرج بزاوية دائرية. في هذه الدراسة، تم استخدام برنامج FLUENT كنوع من Computational Fluid Dynamics (CFD) كنموذج عددي من أجل محاكاة التدفق عبر السدود والتي تحكم من قبل معادلة Reynold averaged Navier Stoke وقورنت النتائج مع النتائج التجريبية. تم استخدام هيكل الشبكة ذو تركيز عال قرب منطقة الجدار في النموذج العددي. طريقة حجم المائع (VOF) وأربعة نماذج من الاضطراب القياسي k–ε ، RNG k–ε ، Realizable k–ε و k–ω القياسية لتخمين شكل السطح الحر. وأظهرت النتائج، ان التدفق على السدود مضطرب وخصائص السطح الحر معقد وغالباً ما يصعب التنبؤ به. أيضا، تم مقارنة شكل المياه السطحية بين القيم التجريبية والقيم العددية التي تم الحصول عليها من نماذج الاضطراب، بينت بانه نموذج k–ε القياسي قد تشابه أفضل ونموذج k–ω كان اقل تشابه مع القيم تجريبية.

## 1. Introduction

Weirs are building for passing water flow in critical conditions or for regulating the water surface level. The most common types of weir crest in the practice are broad

*Corresponding Author thamen92@yahoo.com

crested weir, sharp crested weir and ogee crest weir. These structures which built for measuring the flow in open channels.

The broad crested weir was definition as a flat-crested structure with a length 'L' of crest large enough compared to the flow thickness over crest. The crest is termed broad when the flow streamlines are parallel to the crest and that critical depth is occurred along the crest and the pressure distribution is hydrostatic [1]. Furthermore, the broad crested weir gives it some outstanding characteristics over other forms of weir such as stable overflow pattern, passing of floating debris easily, lower cost of construction and easily designed when compared to other weirs.

In order to prevent erosion and scouring in downstream (D/S) ends of weirs, the hydraulic energy should be dissipated [2], so that the flow characteristics over broad crested weirs were investigated by several investigators with single step of broad crested weir, that's weir called stepped weir.

Based on Bernoulli equation, the flow equation of the weir, which shown in Fig. (1) below, could express the following relationship in Equation (1) between weir discharge and the head over the crest [3];

$$Q=C_d \frac{2}{3}\sqrt{\frac{2}{3}g}\,(H)^{3/2}.\,\mathrm{B} \tag{1}$$

In real fluid, the head above crest of the weir is given by Equation (2);

$$H = h_0 + \frac{Q^2}{2g(H-h_0)^2B^2} \tag{2}$$

The approach velocity ( $V^2/2g$) is very small, so that $h_0$ equal to $H$ in Eq.(1). Eq. (2) becomes as Equation (3);

$$Q = C_d \frac{2}{3}\sqrt{\frac{2}{3}g}\,(h_0)^{3/2}.\,\mathrm{B} \tag{3}$$

Where;

$Q$ = is the actual discharge ( $\mathrm{m}^3/\mathrm{s}$)

$\mathrm{C_d}$ = is the dimensionless coefficient of discharge

$g$ = is the gravitational acceleration($\mathrm{m}/\mathrm{s}^2$)

H = the head above weir crest with approach velocity (m)

$h_0$ = the head above weir crest without approach velocity (m)

B = width of the weir (the perpendicular direction to the flow) (m)

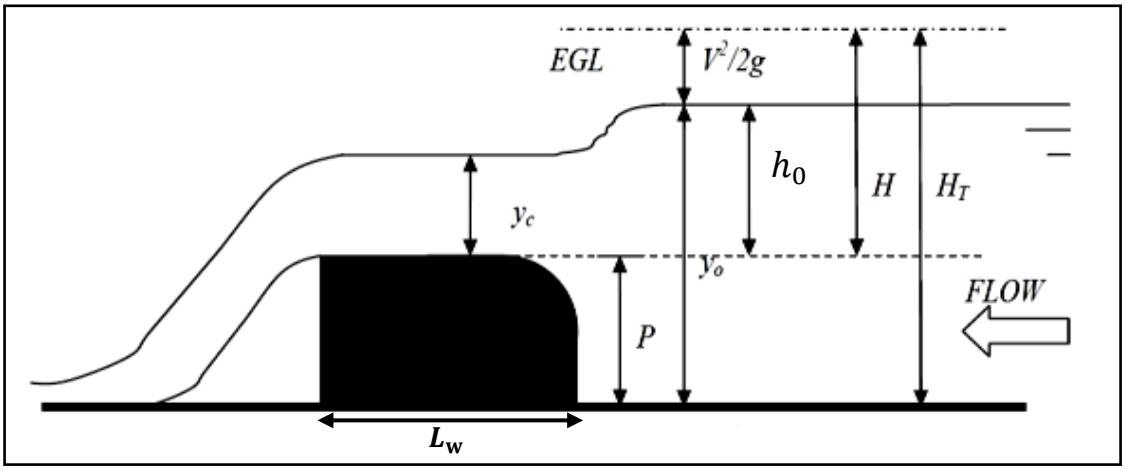


Figure 1. Definition Sketch of a Broad Crested Weir [18]

The characteristics of flow over broad crested weirs and stepped weirs have attracted the attention of many investigators to obtain the flow profile and the coefficient of discharge ($C_d$). The investigating on broad crested weir started by [4] who is presented the first examination on discharge capacity of broad crested weir and developed by many researches as example: [1, 5, 6, 7, 8 and …… etc]. At not a long time ago the researchers studied flow over weir in different shape with numerical and physical methods.

[5] showed that the $C_d$ increases up to 8% if the U/S corner of the weirs is rounded. [9] derived an equation to find $C_d$ for round corner broad crest weir with critical flow condition, assuming $Y_b$= 0.715$Y_c$, where; $Y_c$ = is the critical head and $Y_b$ = is the depth of water at the edge of the weir. The separation at square edge of broad crested weir analyzed by [10] and finding that the length of separation zone is 77% and its height is 15% from the head above crest. The characteristics of square and round edge (R) for rectangular broad crested weirs are studied under free flow and submerged flow conditions by [7]. They found that the best degree of rounding of the U/S weir corner when 0.094 < R/P < 0.250 because this ratio reduces flow separation and it is increasing the $C_d$ values (P= the height of the weir).

The main purpose of broad crested weir is to rise and control U/S water level. In some study a new performance was added to this weir, such [11] changed the shape of traditional broad crested weir by reducing D/S height of the weir to give it a new performance and make it as an energy dissipater. The experimental results showed, reduce in D/S height increased the energy dissipation percent up to 46% in comparison with traditional weirs and $C_d$ was better and gets higher values in comparison with traditional weirs. The authors [12] evaluated the parameters that have effect on the $C_d$ and energy dissipation E% of single step broad crested weir. The results showed that the weir model when the ratio of the length of D/S step to the length of the weir ($L_2/L_1$ =0.5) gives a higher E% in similarity with other weir models.

In recent years, computational fluid dynamics (CFD) has been used to find the flow pattern over weirs. The results have been compared and evaluated against physical model data. [13] simulated a spur dike with free three dimensional (3D) and Reynolds

averaged Naveor Stokes (RANS) equations. The volume of fluid (VOF) and standard k-ε method were used to simulate free surface and turbulence flow. [14] compared the position of the free surface profile over a laboratory rectangular broad crested weir with numerical CFD model. For the smaller flow rate they measured, the results showed that the prediction of the U/S water depth was excellent and the rapidly varied flow profile over the crest and a stationary wave profile was observed at D/S, where the flow was supercritical.

The velocity and pressure measurements were studied numerically by [8] on broad crested weir. Pressure and velocity distributions measurements were conducted systematically and they showed the rapid redistributions of both velocity and pressure fields at the U/S end of the weir crest. [15] describes the validation of CFD for free surface flows over broad crested weir by using a published experimental dataset of [21] and discusses the accuracy of CFD in being able to predict the free surface profile. The study of [16] on a broad crested weir with a rounded corner is presented to investigate the free surface profile of water by using the volume of fluid (VOF). The computational results showed a good agreement with experimental result obtained in the laboratory. [17] employed CFD model on triangular broad crested weir to investigate the flow pattern over it. VOF with the RNG $k$ -ε, standard $k$ -ε and the large eddy simulation (LES) were applied to find the water level profile and showed the RNG $k$ -ε model has the maximum accuracy with experimental data in comparison with other turbulence models used. In the study of [18], laboratory model with CFD model was carried out on broad crested weir located on rectangular channel to predict the $C_d$ value. Good agreements between the laboratory value and the CFD value were obtained. The mean relative error percentage (RE), root mean square errors (RMSE) and mean absolute errors (MAE) for the $C_d$ are 3.043, 0.123 and 0.0987 respectively. The effect of inclination from 90º to 23º weir in the U/S face of rectangular broad crested weirs and flow characteristic is studied by [19] by using CFD model together with laboratory model were applied to improve the performance of broad crested weirs in order to reduce the effect of flow separation. Also the results showed, by decreasing the slope of the U/S side, the discharge efficiency increased with slope of 23º about 22% higher than the standard weir.

The objective of this study are to examine the laboratory measurements and 2D numerical modeling which employed to simulate the flow pattern over a rectangular broad crested weir and stepped weir located in a rectangular channel and comparison between free surface profiles obtained from experiment and numerical results for different turbulent models.

## 2. Experimental Work

The experiments tests were carried out in the Hydraulic Engineering Laboratory, Department of Environmental Engineering, Collage of Engineering, Al-Mustansiriayah University in Baghdad. In this research, the flume that was made of glass with a cross section of 0.3 m wide, 0.3 m deep and 4.8 m long was shown in photo (A) and photo (B). The broad crested weir was 0.15 m of height (P), 0.3 m of width (B) and as 0.36 m

long (L), while a stepped weir 0.15 m of height (P), 0.3 m width (B) and 0.4 m total length (L), while the height of step (P2) is 0.075 m. The two weirs have a rounded edge at U/S corner, which the radius (R) of rounded corner 0.02 m, in order to reduce the adverse effects of separations zone. This radius determined according to the design criteria suggested by [7], the shapes of weirs shown in Fig. (2). Water was supplied from the pump located at storage tank through a supply pipe from this tank and controlled by an inlet valve for regulating the pumped water flow from its storage tank into the rectangular flume. At the top of flume sides, three movable point gauges of 1 mm accuracy were installed along the centerline of the flume for water level measurements and traverse apparatus at different static points spaced.

Photo A. The Laboratory Flume with Broad Crested Weir

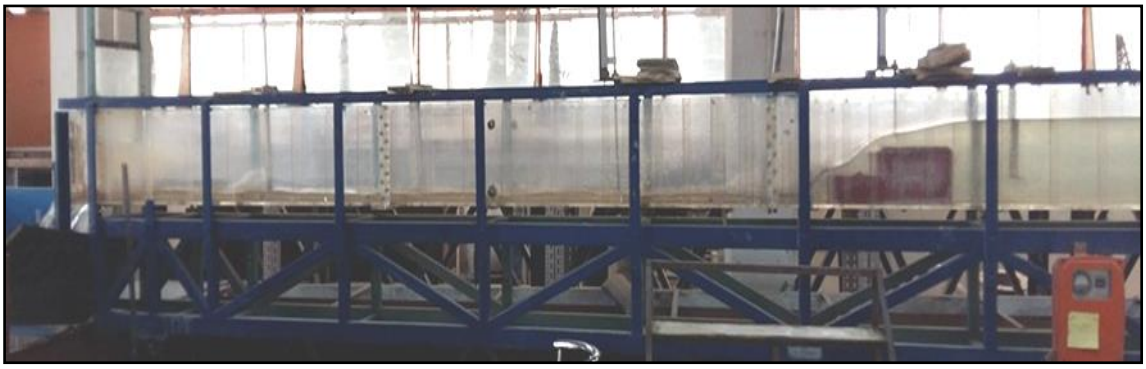

Photo A. The Laboratory Flume with Broad Crested Weir

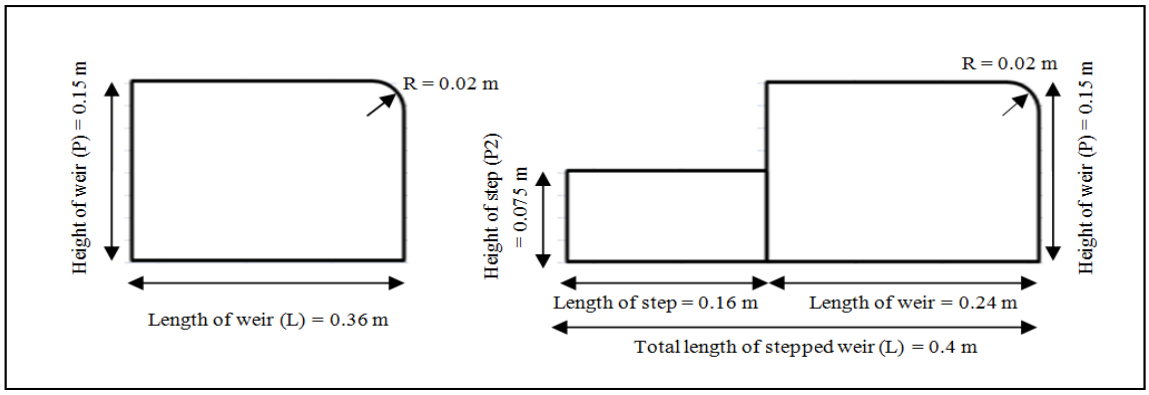


Figure 2. Definition Sketch for Broad Crested Weir and Stepped Weir

## 3. Numerical Modeling

Analysis of flow over the weirs is an important engineering problem. So, new developments in computer science and numerical techniques have advanced the use of CFD as a controlling tool for this purpose**.** In this research, numerical modeling was done using FLUENT program. FLUENT is one of the great and common CFD commercial software, it has the capacity to solve 2D and 3D problems of open channel flow and it has able to predict flow profile over weirs. It uses volume of fluid (VOF) method to determine the water level in each cell, which is used in many hydraulic problems. [22] VOF represent the sharp interface between the air and water phases. A flow which consists of two immiscible phases, in this case water and air is called a multi-phase flow. With the VOF model, the location and shape of the interface also known as the free surface profile can be determined.

The governing equations of numerical modeling in FLUENT software for unsteady incompressible 2D flows over weirs are continuity and Navier-Stokes equations, which are based on principles of physics mass conservation and Newton's Second Law within a moving fluid. The continuity and Navier-Stokes equations are described by the differential Equation (4) and (5) respectively [23];

$$\frac{\partial \rho}{\partial t} + \frac{\partial}{\partial x_i}(\rho u_i) = 0 \tag{4}$$

$$\frac{\partial}{\partial t}(\rho u_i) + \frac{\partial}{\partial x_i}(\rho u_i u_j) = -\frac{\partial P}{\partial x_i} + \frac{\partial}{\partial x_i}\left[\mu\left(\frac{\partial u_i}{\partial u_j} + \frac{\partial u_j}{\partial x_i}\right)\right] + \rho g_i + \vec{F} \tag{5}$$

Where: ρ = fluid density, $u_{i,j}$= velocity in X and Y direction, x = space dimensions, t = time, p = the pressure, μ = $\mu_0 + \mu_t$, $\mu_0$ is dynamic viscosity and $\mu_t$ is turbulence viscosity, $g_i$ = acceleration due to gravity and $\vec{F}$ = the body force.

## 4. Turbulence Models

Turbulent flows are characterized by fluctuating velocity. These fluctuations mix transported quantities such as momentum, energy, kinetic energy and species concentration, and cause the transported quantities to fluctuate as well. Since these fluctuations can be of small scale and high frequency, they are also computationally expensive to simulate directly in practical engineering calculations. Instead, the exact governing equations can be time-averaged, ensemble-averaged, or otherwise manipulated to remove the small scales, resulting in a modified set of equations that are computationally less expensive to solve and describe it [24].

Turbulent models have been classified based on [25] to one eq. model, two eq. model and Re. stress model. The models has also been divided into the following classes: k – ε model (standard k – ε model, renormalization group (RNG) k – ε model and realizable k – ε model) and k – ω model (standard k – ω and shear stress transport (sst) k –ω).

### 4.1 *k – ε Turbulence models*

#### 4.1.1 *The Standard k – ε Turbulence model*

In the derivation of the standard (k-ε) model, it is assumed that the flow is fully turbulent, and the effects of molecular viscosity are negligible. The standard (k-ε) model is; therefore, valid only for fully turbulent flows. The two-dimensional governing equations of turbulent kinetic energy and turbulent energy dissipation rate by using the standard (*k*–ε) model are as follows[26];

$$\frac{\partial}{\partial t}(\rho k)+\frac{\partial k}{\partial x_i}(\rho k u_i)=\frac{\partial}{\partial x_j}\left[\left(\mu+\frac{\mu_t}{\sigma_k}\right)\frac{\partial k}{\partial x_i}\right]+G_k-\rho\varepsilon \tag{6}$$

$$\frac{\partial}{\partial t}(\rho \varepsilon)+\frac{\partial \varepsilon}{\partial x_i}(\rho \varepsilon u_i)=\frac{\partial}{\partial x_j}\left[\left(\mu+\frac{\mu_t}{\sigma_\varepsilon}\right)\frac{\partial \varepsilon}{\partial x_i}\right]+G_{1\varepsilon}\frac{\varepsilon}{k}G_k-G_{2\varepsilon}\rho\frac{\varepsilon^2}{k} \tag{7}$$

Where the eddy viscosity $\mu_t$, is computed by combining the turbulent kinetic energy (k) and rate of dissipation (ε), as follows in Equation (8);

$$\mu_t=C_\mu\,\rho\frac{k^2}{\varepsilon} \tag{8}$$

In above Equations, $G_{1\varepsilon}$, $G_{2\varepsilon}$, and $C_\mu$ are constants and equal to 1.44, 1.92, and 0.09, respectively. $\sigma_k$ and $\sigma_\varepsilon$ are the turbulent Prandtl Numbers for *k* and ε equal to 1.0, 1.3, respectively [26].

#### 4.1.2 *The RNG k - ε Turbulence Model*

The RNG (k-ε) turbulence model is derived from the instantaneous Navier-Stokes equations, from using a mathematical technique called, "renormalization group" (RNG) methods. The analytical derivation results in a RNG model with constants different from those in the standard (k-ε) model and additional terms and functions in the transport equations for k and ε,[27].

$$\frac{\partial}{\partial t}(\rho k)+\frac{\partial k}{\partial x_i}(\rho k u_i)=\frac{\partial}{\partial x_j}\left[\left(a_k\mu_{\varepsilon ff}\right)\frac{\partial k}{\partial x_i}\right]+G_k-\rho\varepsilon \tag{9}$$

$$\frac{\partial}{\partial t}(\rho \varepsilon)+\frac{\partial k}{\partial x_i}(\rho \varepsilon u_i)=\frac{\partial}{\partial x_j}\left[\left(a_\varepsilon\mu_{\varepsilon ff}\right)\frac{\partial \varepsilon}{\partial x_i}\right]+G_{1\varepsilon}\frac{\varepsilon}{k}G_k-G^*{}_{2\varepsilon}\rho\frac{\varepsilon^2}{k} \tag{10}$$

$$G^*{}_{2\varepsilon}=G_{2\varepsilon}+\frac{c_\mu\,\rho\eta^3\left(1-\frac{\eta}{\eta_0}\right)}{1+ß\eta^3} \tag{11}$$

$$\eta=\frac{sk}{\varepsilon} \tag{12}$$

In above Equations, $G_{1\varepsilon}$, $G_{2\varepsilon}$, and $C_\mu$ are constants and equal to 1.42, 1.68, and 0.0845, respectively. $a_k$ and $a_\varepsilon$ equal to 1.393, $\eta_0$ equal to 4.38, $\mu_{\varepsilon ff}$ equal to 1 and ß equal to 0.012 [27].

### **4.1.3** *The Realizable k - ε Turbulence Model*

The realizable (k-ε) model is one of turbulent model can be used in special case. The term "realizable" refers that the model satisfies certain mathematical constraints on the normal stresses, consistent with the physics of turbulent flows. To understand this, consider combining the Boussinesq relationship and the eddy viscosity definition to get the following expression for the normal Reynolds stress in an incompressible strained mean flow [28].

$$\frac{\partial}{\partial t}(\rho k)+\frac{\partial k}{\partial x_i}(\rho k u_i)=\frac{\partial}{\partial x_j}\left[\left(\mu+\frac{\mu_t}{\sigma_k}\right)\frac{\partial k}{\partial x_i}\right]+G_k-\rho\varepsilon \tag{13}$$

$$\frac{\partial}{\partial t}(\rho \varepsilon)+\frac{\partial \varepsilon}{\partial x_i}(\rho \varepsilon u_i)=\frac{\partial}{\partial x_j}\left[\left(\mu+\frac{\mu_t}{\sigma_\varepsilon}\right)\frac{\partial \varepsilon}{\partial x_i}\right]+\rho C_1 S_\varepsilon-\rho C_2\frac{\mathrm{E}^2}{k+\sqrt{\nu\varepsilon}} \tag{14}$$

$$C_1=\max.\left[0.43,\frac{\eta}{\eta+5}\right],\ \eta=\frac{sk}{\varepsilon} \tag{15}$$

$$\mu_t=C_\mu\,\rho\frac{k^2}{\varepsilon} \tag{16}$$

In above Equations, $G_{1\varepsilon}$ and $G_{2\varepsilon}$ equal to 1.44 and 1.9, respectively. $\sigma_k$ and $\sigma_\varepsilon$ equal to 1 and 1.2.

The term *Gk*, representing the production of turbulent kinetic energy, is modeled identically for the standard *k* - *ε*, RNG *k* - *ε*, and realizable *k* - *ε* models. From the exact equation for the transport of *k*, this term can be defined as [29]:

$$G_k=-\rho\,\overline{\acute{u}_i\acute{u}_j}\frac{\partial u_i}{\partial x_i} \tag{17}$$

### **4.2. The Standard k - ω Turbulence Model**

$$\frac{\partial k}{\partial t}+u_j\frac{\partial k}{\partial x_j}=\frac{1}{\rho}\tau_{ij}\frac{\partial u_i}{\partial x_j}-ß^*k\omega \tag{18}$$

$$\frac{\partial \omega}{\partial t}+u_j\frac{\partial \omega}{\partial x_j}=\frac{\omega}{\rho k}\boldsymbol{\tau}_{ij}\frac{\partial u_i}{\partial x_j}-ßk\omega^2+\frac{1}{\rho}\frac{\partial}{\partial x_j}\left[(\mu+\sigma\mu_t)\frac{\partial \omega}{\partial x_j}\right] \tag{19}$$

## **5. Analysis Method**

FLUENT can handle a number of different grid topologies. For this purpose, GAMBIT used to produce the geometry of model and to create mesh. GAMBIT can be created 2D and 3D structured/unstructured/mix grids. The mesh used in this study as shown in Fig. (3). Grid size of modeling is an important part of the numerical simulation because affect not only the accuracy of the result, but also on the simulation time. However, when the mesh size becomes smaller and fine, the total mesh number increases and more computational time needed, so increasing mesh number gives better results**.** Consequently, to choose the optimum cell size, the mesh with difference dimension in edge and face is used. The mesh sizes with 2 mm for edge and 4.5 mm for face are employed.

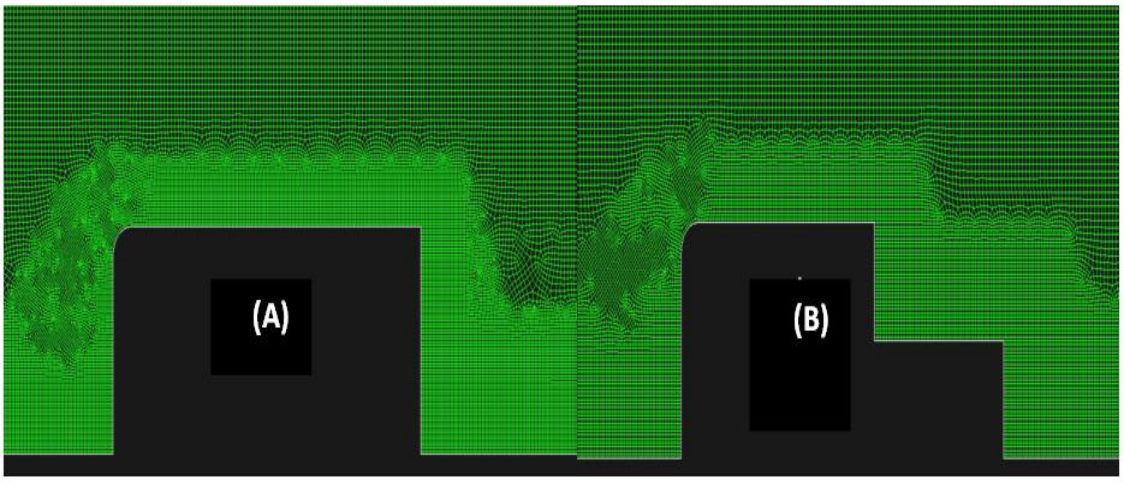


Figure 3. Zoomed Grid near the (A) Broad Crested Weir and (B) Stepped Weir

Boundary conditions one of the most important order of the numerical analysis of flow field to determine the boundaries of the numerical model, which are matched appropriately with the physical conditions of the problem. In this study for numerical modeling of weirs, the boundary conditions of the Fig. (4) have been provided. According to figure (4), the original boundary conditions of flow over weir include inlet (pressure inlet for water and pressure inlet for air), outlet (pressure outlet), wall (wall) and Symmetry (free surface).

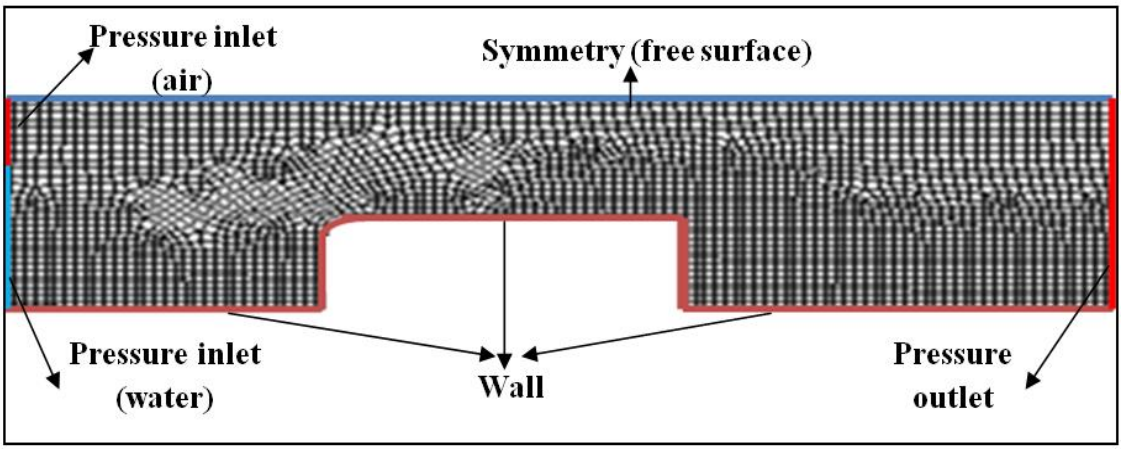


Figure 4. Boundary Condition using Gambit Model

The first step of the solution in the FLUENT software is checking the mesh and it is generally a good idea to check their mesh right after solving it, in order to detect any mesh trouble before get started with the problem of flow and it represent the verification of the accuracy of meshing. Before iterating, the flow must be initialized to provide initial point for the solution. The solution will stop automatically when each variable meets its specified convergence measure and the message is (the solution is convergences). When the convergence checks that mean the value is constant even we increased the iterate and the number of iterations was optimum.

## 6. Results and Discussion

To have access to an appropriate turbulence model for simulation the free surface profile over weirs, numerical model is applied with different models of turbulence (standard k – ε model, RNG k – ε model, realizable k – ε model and standard k – ω model) under the same conditions (boundary condition, material, mesh and...etc.). Then, these turbulence model can be accessed in comparison with laboratory model. The flow profile over broad crested weir by using different turbulent model as shown in Figures (5, 6, 7 and 8) and Figures (9, 10, 11 and 12) for stepped weir.

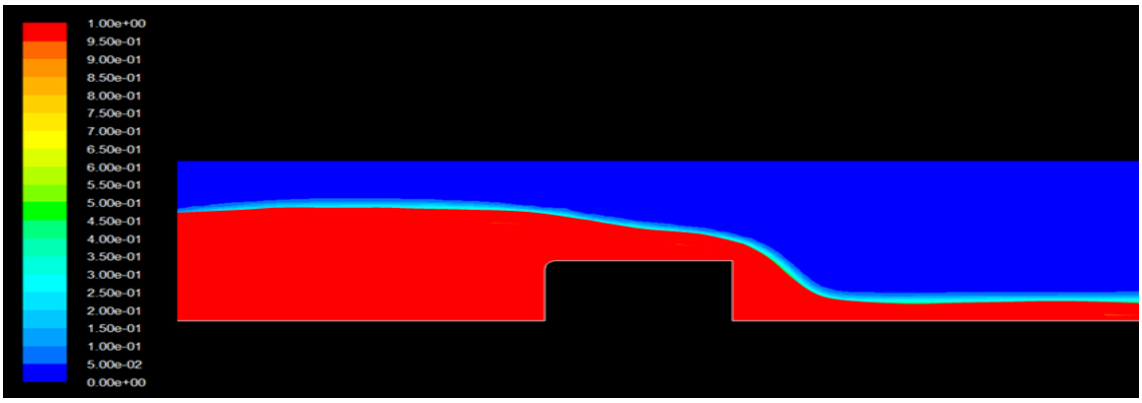


Figure 5. Numerical Water Surface Profile Contours over a Broad Crested Weir by Standard k- ε model

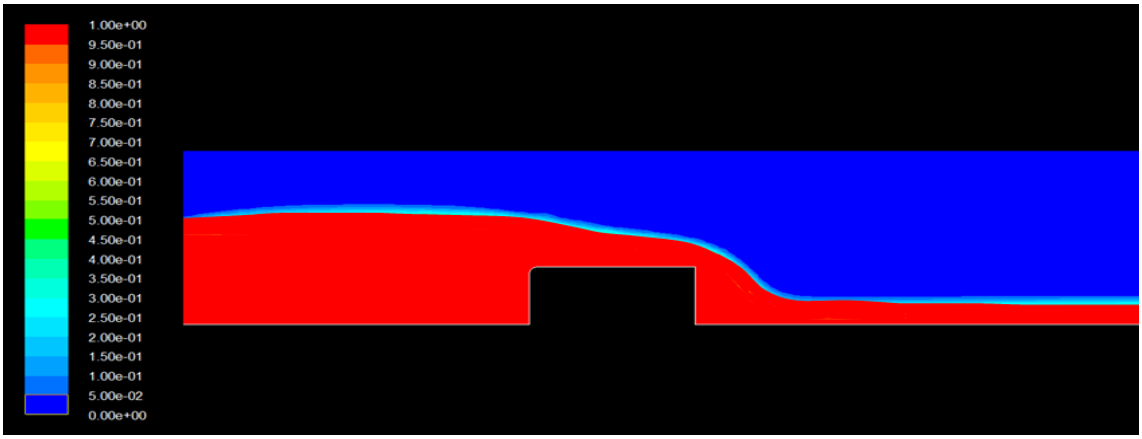


Figure 6. Numerical Water Surface Profile Contours over a Broad Crested Weir by RNG k- ε model

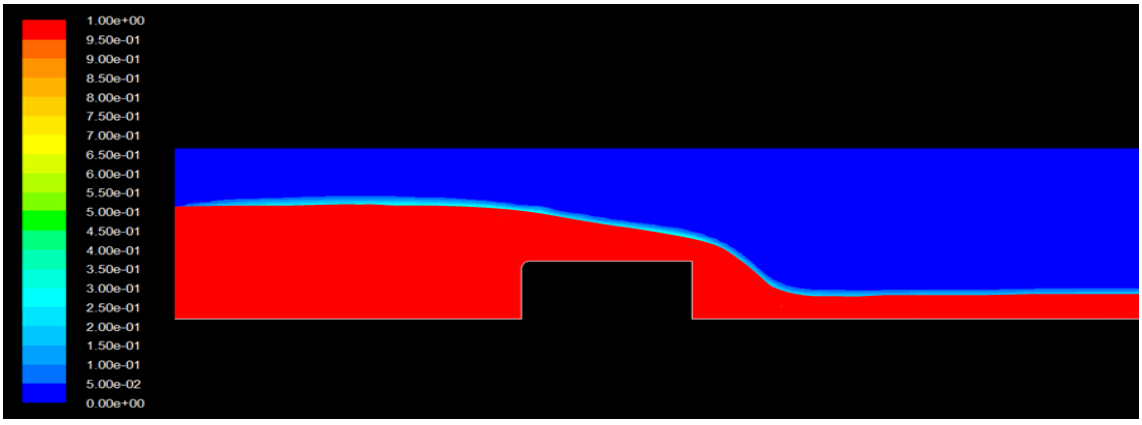


Figure 7. Numerical Water Surface Profile Contours over a Broad Crested Weir by Realizable k- ε model

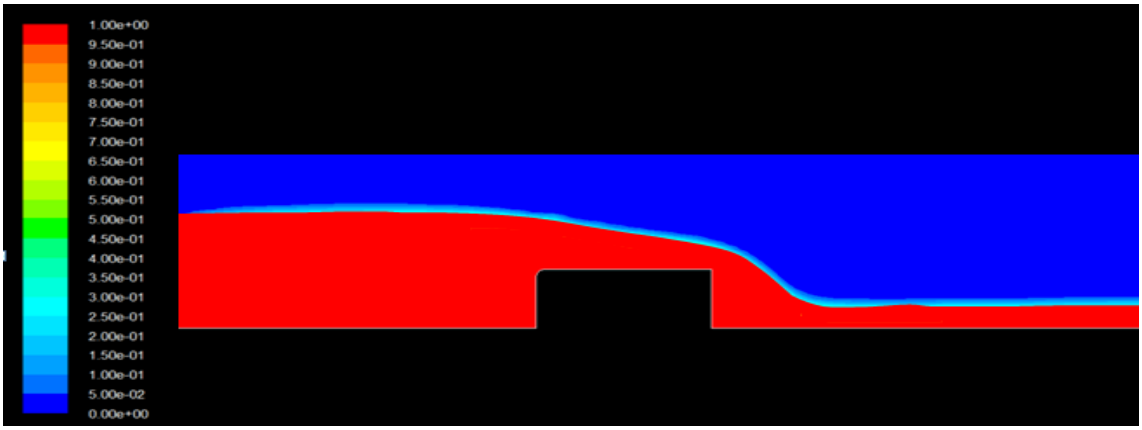


Figure 8. Numerical Water Surface Profile Contours over a Broad Crested Weir by standard k – ω model

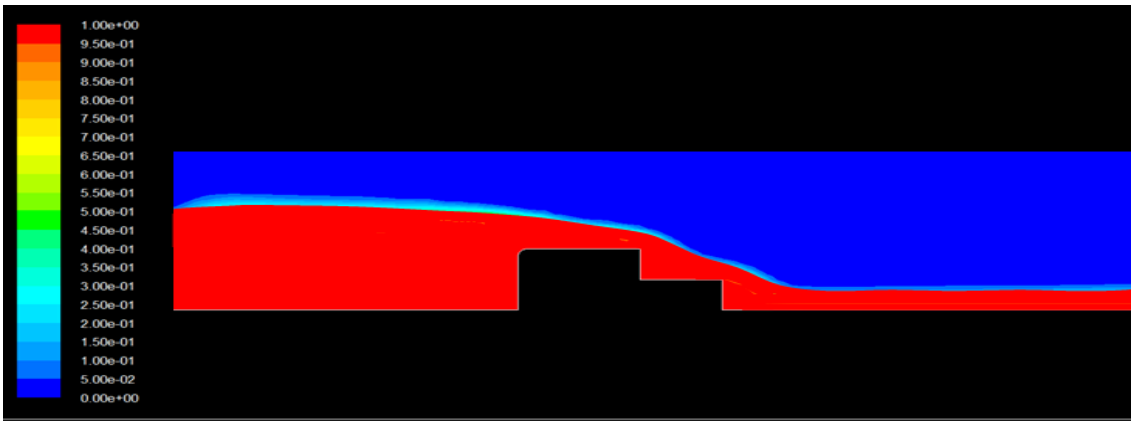


Figure 9. Numerical Water Surface Profile Contours over a Stepped Weir by Standard k- ε model

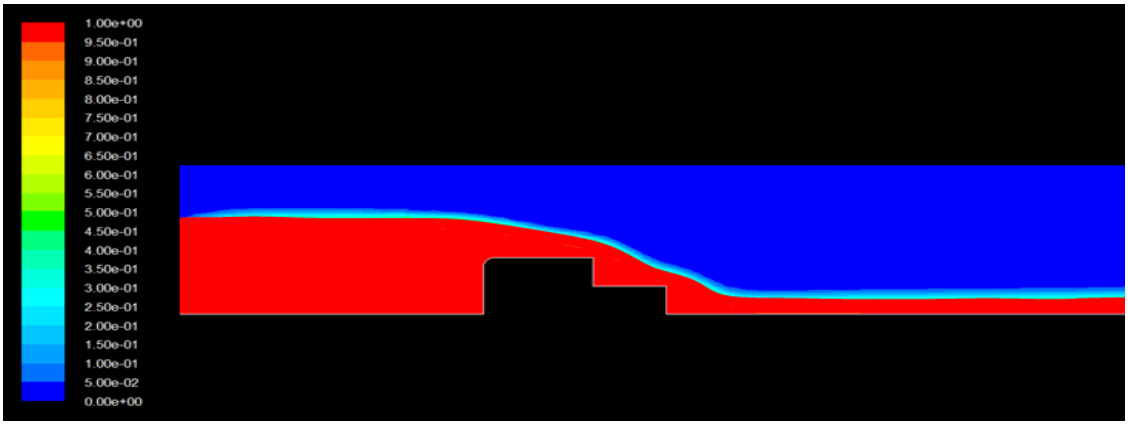


Figure 10. Numerical Water Surface Profile Contours over a Stepped Weir by RNG k- ε model

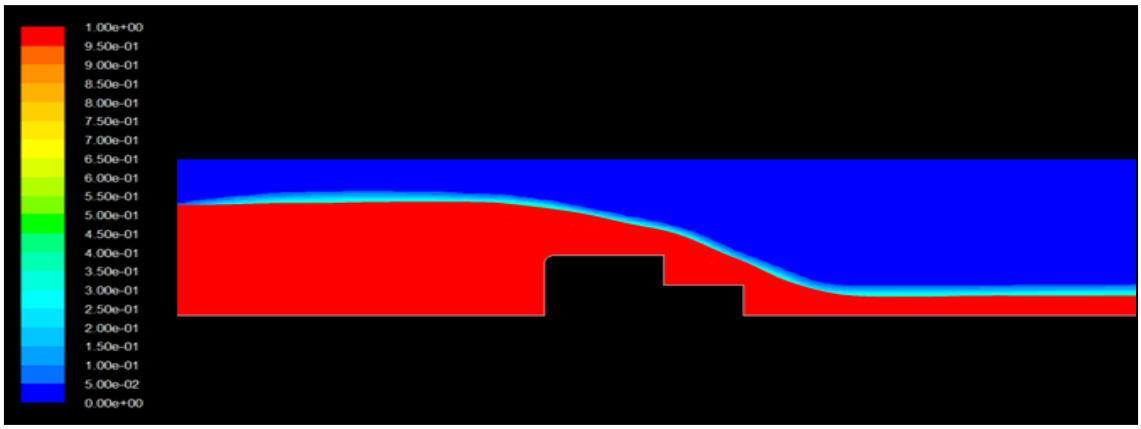


Figure 11. Numerical Water Surface Profile Contours over a Stepped Weir by Realizable k- ε model

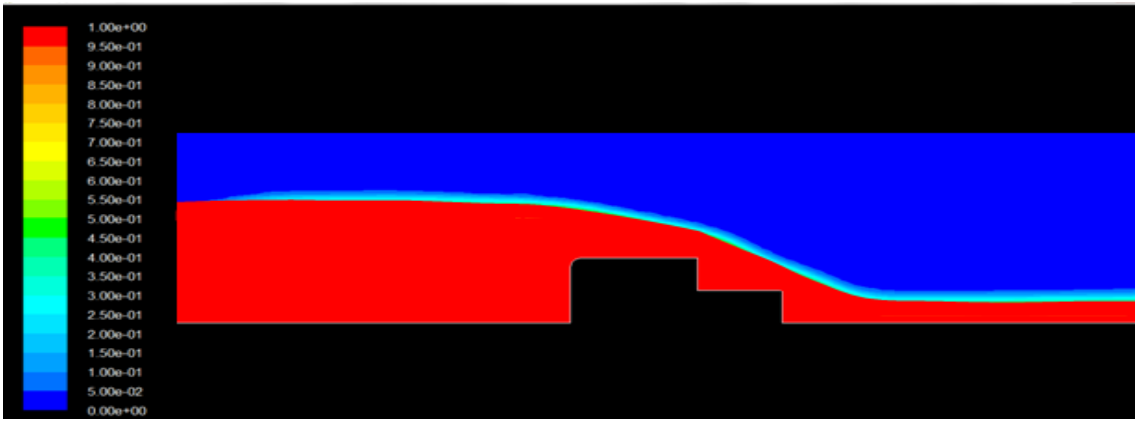


Figure 12. Numerical Water Surface Profile Contours over a Stepped Weir by standard k – ω model

The flow profile over broad crested weir and stepped weir by using different turbulent model and experimental model shown in Figs. (13) and Figs. (14) respectively**,** which indicates a comparison of water surface profile between experimental data and predicted value obtained from the standard k–ε, RNG k–ε, realizable k–ε and standard k–ω. Based on two figures, the water level along the flow direction gradually decreasing until reaches stability condition in D/S of the flume and the standard k–ε model has the best similarity with experimental data and standard k–ω model has the minimum similarity with experimental data. As showed in a figure below by XY plot for all tests the definition of X and Y, are X is the horizontal distance of the channel and Y is the depth of flow along the channel, where x = 0.9 m was represented the entry depth on weir.

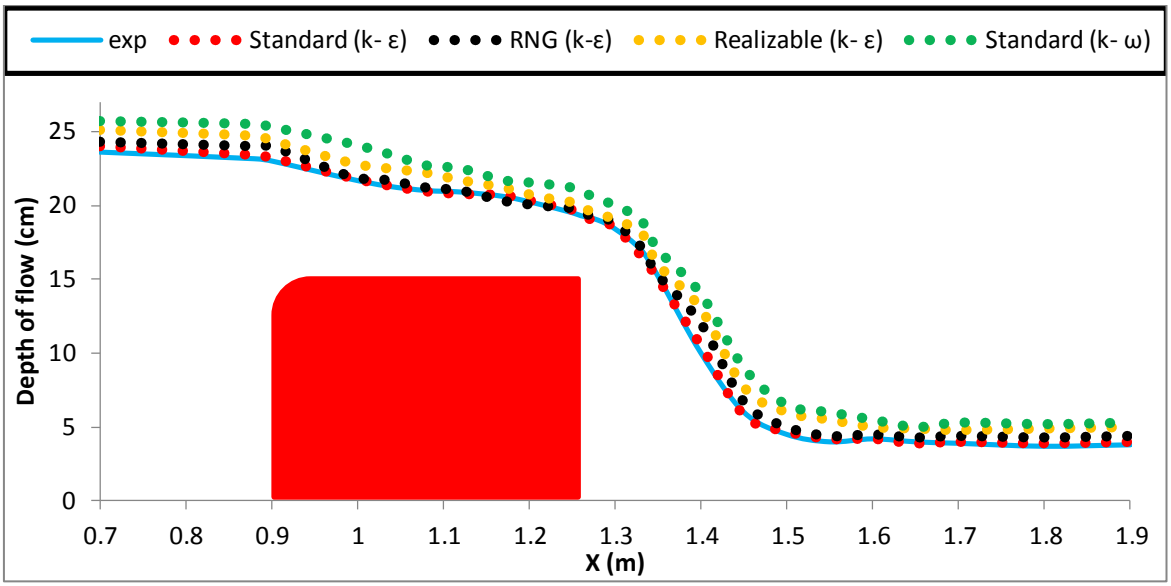


Figure 13. Comparison between Exp. and Num. Method of Water Surface Profile over Broad Crested Weir for Different Turbulent Models

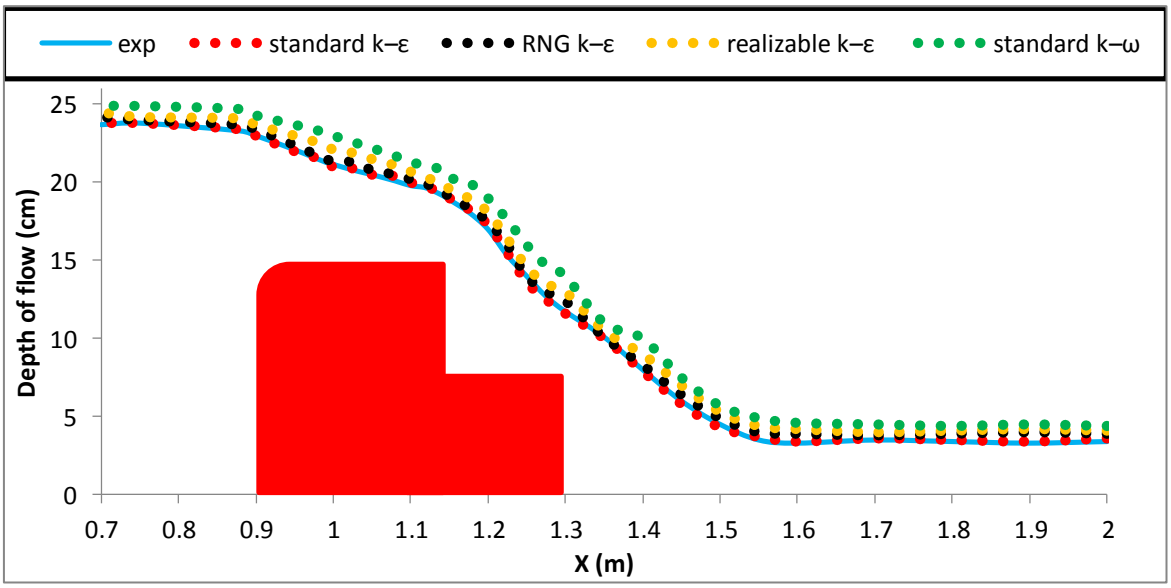


Figure 14. Comparison between Exp. and Num. Method of Water Surface Profile over Stepped Weir for Different Turbulent Models

To test any turbulent model is the best and worst simulated flow profile in this study, the relative error of water level (the difference between results obtained from the numerical and experimental models) for above figures are shown in Table (1) for broad crested weir and stepped weir.

The relative error between experimental and numerical result by the mean relative error percentage (RE), root mean square errors (RMSE) and mean absolute errors (MAE) were used to evaluate the result accuracies. The RE, RMSE and MAE are defined as:

$$RE = \frac{100}{N} \sum_{i=1}^{N} \left| \frac{h_{exp.} - h_{num.}}{h_{exp.}} \right| \quad (20)$$

$$RMSE = \sqrt{\frac{1}{N}\sum_{i=1}^{N}(h_{exp.} - h_{num.})^2} \quad (21)$$

$$MAE = \frac{1}{N}\sum_{i=1}^{N}\left|h_{exp.} - h_{num.}\right| \quad (22)$$

Where; $h_{exp.}$ is the experimental head, $h_{num.}$ is the numerical head, N is the total number of points and i is the number of points. The relative error for broad crested weir was about 5.11% to 13.1 % in RE, 0.39 % to 1.97 % in RMSE and 0.29 % to 1.86 % in MAE. While, the relative error for stepped weir was about 3.54 % to 11.79 % in RE, 0.17 % to 1.59 % in RMSE and 0.149 % to 1.53 % in MAE.

Table 1. Relative Error of Water Level on Broad Crested Weir and Stepped Weir

| Relative Error of Water level to Broad Crested Weir | | | |
|---|---|---|---|
| *Turbulent model* | *Equation* | | |
| | *RE%* | *RMSE%* | *MAE%* |
| standard k–ε | 5.11 | 0.39 | 0.29 |
| RNG k–ε | 5.25 | 0.43 | 0.36 |
| realizable k–ε | 8.37 | 1.23 | 1.08 |
| standard k–ω | 13.1 | 1.97 | 1.86 |
| *Relative Error of Water level to Stepped Weir* | | | |
| *Turbulent model* | *Equation* | | |
| | *RE%* | *RMSE%* | *MAE%* |
| standard k–ε | 3.54 | 0.17 | 0.146 |
| RNG k–ε | 4.63 | 0.39 | 0.35 |
| realizable k–ε | 7.86 | 0.83 | 0.8 |
| standard k–ω | 11.79 | 1.59 | 1.53 |

For example, the relative error of water level (head) at x =0. 7 as follows; the Standard k– ε model have the minimum error value was 1.7% and the Standard k- ω model have the maximum error value was 8% for broad crested weir as shown in Table (2) and Fig. (15), while for the stepped weir as follows; the Standard k– ε model have the minimum error value was 1.27% and the Standard k- ω model have the maximum error value was 6% as shown in Table (3) and Fig. (16).

Table 2. Relative Errors of the Head between Num. and Exp. Models for Broad Crested Weir

| *Turbulent Model* | *Standard k- ε* | *RNG k- ε* | *Realizable k- ε* | *Standard k- ω* |
|---|---|---|---|---|
| $H_{exp.}$ | 23.6 | 23.6 | 23.6 | 23.6 |
| $H_{num.}$ | 24 | 24.3 | 25.1 | 25.5 |
| RE % | 1.7 | 3 | 6.5 | 8 |

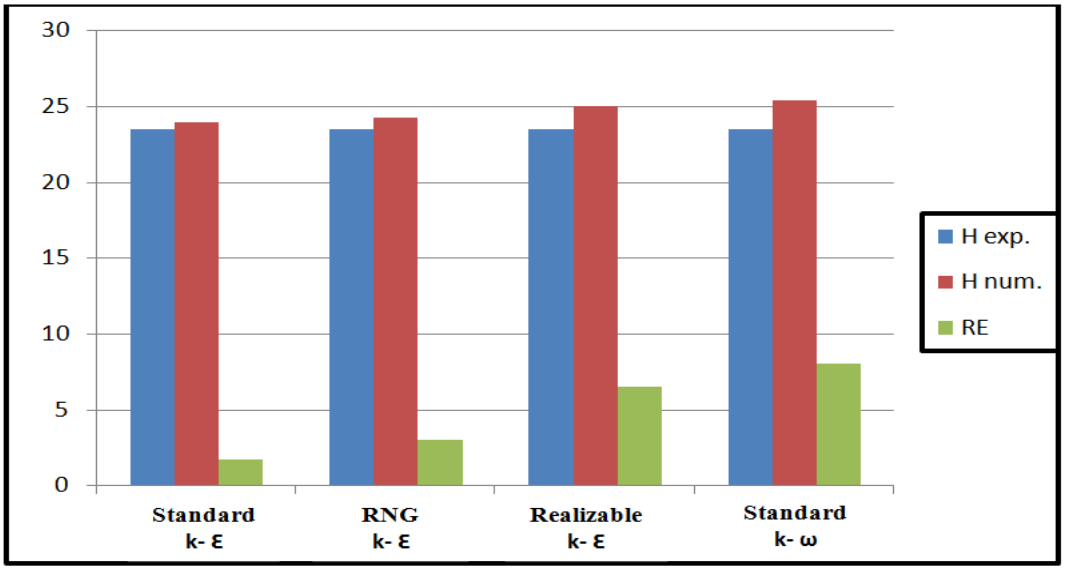


Figure 15. Relative Errors for Head Resulting from Applying Different Turbulent Models for Broad Crested Weir

Table 3. Relative Errors of the Head between Num. and Exp. Models for Stepped Weir

| *Turbulent Model* | *Standard k- ε* | *RNG k- ε* | *Realizable k- ε* | *Standard k- ω* |
|---|---|---|---|---|
| $H_{exp.}$ | 23.5 | 23.5 | 23.5 | 23.5 |
| $H_{num.}$ | 23.8 | 24.2 | 24.5 | 24.9 |
| RE % | 1.27 | 2.9 | 4.26 | 6 |

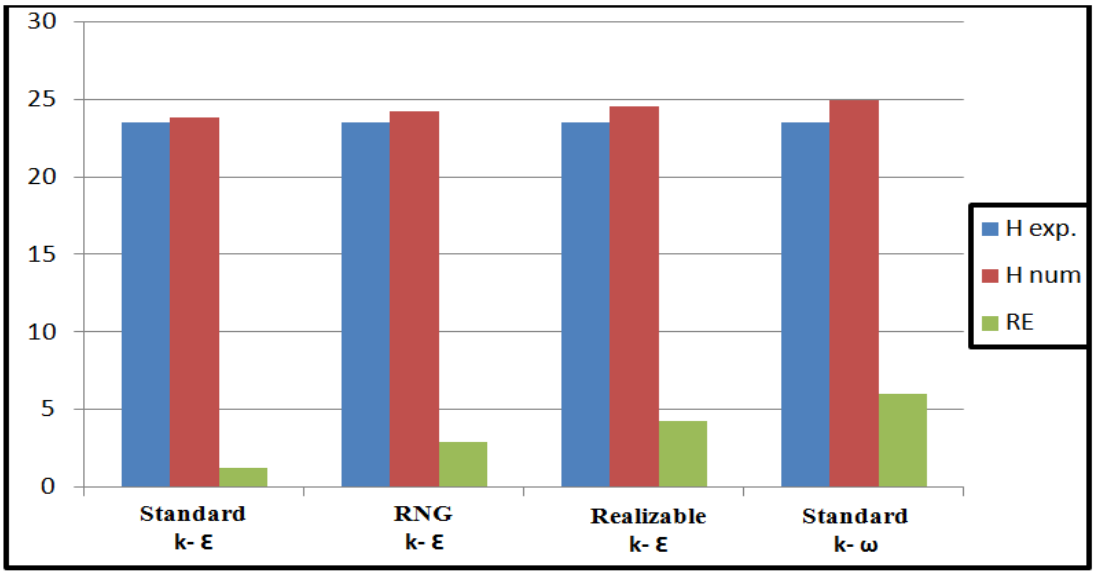


Figure 16. Relative Errors for Head Resulting from Applying Different Turbulent Models for Stepped Weir

## 7. Conclusion

In the present numerical study, flow over broad crested weir and stepped weir was simulated by using 2D code (FLUENT software). The different turbulence models (Standard k-ε, RNG k-ε, Realizable k-ε and Standard k- ω) with different mesh for face

and edge can simulate the flow successfully. The VOF method was used to predict the water surface profile. Results obtained in this study showed that the water level along the flow direction gradually decreasing until reaches stability condition in D/S of the flume and the comparison of water surface profile between experimental data and predicted value obtained from the turbulent models showed that the standard k–ε model has the best similarity with experimental data and standard k–ω model has the minimum similarity with experimental data. The relative error of water level between experimental and standard k–ε model for broad crested weir was 5.11% in RE and standard k–ω was 13.1% in RE, while, the relative error of water level between experimental and standard k–ε model for stepped broad crested weir was 3.54% in RE and standard k–ω was 11.79% in RE. Also this study investigation the relative error of water level at x =0. 7 and find the standard k– ε model have the minimum error value in two weirs.

## Abbreviations

A list of symbols that used in this research, shown in table below.

| | |
|---|---|
| $C_d$ | the coefficient of discharge |
| $h_{exp.}$ | the experimental head |
| $h_{num.}$ | the numerical head |
| $L_2$ | the length of D/S step |
| $Y_b$ | the depth of water at the edge of the weir |
| $Y_c$ | the critical head |
| B | width of the weir |
| E% | the energy dissipation |
| Fr | the dimensionless Froude number |
| H | the head above weir crest with approach |
| h, $h_0$ | the head above weir crest without approach |
| L, $L_1$ | the length of the weir |
| P | the height of the weir |
| P2 | height of step |
| R | round edge of upstream edge |
| $Q$ | the actual discharge |
| $g$ | the gravitational acceleration |

## 8. References

1. Chow, V. T. (1959). "Open channel hydraulics", New York, McGraw-Hill, 1959.
2. Chanson H., (2001). "Hydraulic Design of Stepped Spillways and Downstream Energy Dissipaters", Dam Engineering, Vol. 11, No. 4, pp. 205-242..
3. Boiten W., (2002). "Flow Measurement Structures", Wageningen University, Wageningen, Gelderland, Netherlands, Flow Measurement and Instrumentation, Vol. 13, No. 5, pp. 203-207.
4. Bazin, (1896). "Open Channel Hydraulics", USA, McGraw-Hill,

5. Woodburn J. G., (1932). "Tests of Broad-Crested Weirs", Transactions of the American Society of Civil Engineers, Vol. 96, No.1, pp. 417-453.
6. Hall G. W., (1962). "Discharge Characteristics of Broad-Crested Weirs Using Boundary Layer Theory", London, England, Proceedings of the Institution of Civil Engineers, pp. 172-190.
7. Ramamurthy A. S., Tim U. S., and Rao M. J., (1988). "Characteristics of Square-Edged and Round-Nosed Broad-Crested Weirs", Journal of Irrigation and Drainage Engineering, Vol. 114, No. 1, pp. 61-73.
8. Gonzalez, C. A., and Chanson, H. (2007). "Experimental measurements of velocity and pressure distribution on a large broad-crested weir", Australia, Flow Measurement and Instrumentation, Vol. 18, pp. 107–113.
9. Henderson F. M., (1966). "Open Channel Flow", New York, MacMillan.
10. Moss W. D., (1972). "Flow Separation at the Upstream of a Square-Edged Broad-Crested Weir", Journal of Fluid Mechanics, Vol. 52, No. 2, pp. 307-320.
11. Hussein H. H., Juma A. and Shareef S., (2009). "Flow characteristics and energy dissipation over stepped round–nosed broad–crested weirs", University of Mosul, Journal of Al-Rafidain Engineering.
12. Hamid H., Inam A. K. and Saleh J. S., (2010). "Improving the Hydraulic Performance of Single Step Broad-Crested Weirs", University of Mosul, Iraqi, Journal of Civil Engineering, Vol. 7, No. 1, pp. 1-12.
13. Yazdi, J., Sarkardeh, H., Azamathulla, H.M., Ghani, A.A., (2010). "3D simulation of flow around a single spur dike with free surface flow", Int. J. River Basin Manage. No. 8 pp. 55-62.
14. Sarkar M. A. and Rhodes. D. G., (2004). "CFD and physical modeling of free surface over broad-crested weir", Cranfield University, Swindon, pp. 215–219.
15. Hargreaves D. M., Morvan H. P. and Wright N. G., (2007). "Validation of the Volume of Fluid Method for Free Surface Calculation: The Broad-Crested Weir", The University of Nottingham, Engineering Applications of Computational Fluid Mechanics, Vol. 1, No. 2, pp. 136–146.
16. Afshar H. and Hooman H., (2013), "Experimental and 3-D numerical simulation of flow over a rectangular broad-crested weir", International Journal of Engineering and Advanced Technology, Vol. 2, No. 6, pp. 214-219.
17. Hooman S., (2014). "3D Simulation Broad of Flow over a Triangular Broad-Crested Weir", Journal of River Engineering, Vol. 2, No 2.
18. Seyed H. and Hossein A., (2014). "Flow over a Broad-Crested Weir in Subcritical Flow Conditions, Physical Study", Journal of River Engineering, Vol. 2, No. 1.
19. Al-Hashimi A. S., Sadeq A. and Huda M., (2015). "Determination of Discharge Coefficient of Rectangular Broad-Crested Weir by CFD", The 2nd International Conference of Construction.
20. Dias, F., Keller, J.B., and Broeck,J.M, (1988). "Flows over rectangular weirs", Phys. Fluids, No. 31, pp. 2071–2076.
21. Hager W. H. and Schwalt M., (1994). "Broad-crested weir", Journal of Irrigation and Drainage Engineering, Vol. 120, No. 1, pp.13-26.

22. Hirt C. W. and Nichols B. D., (1981). "Volume of flu*id (VOF) method for the dynamics of free boundaries*", Journal of Computational Physics, Vol. 39, No. 1, pp. 201-225.
23. Liu C, Hute A. and Wenju M., (2002). "*Numerical and experimental investigation of flow over a semicircular weir*", Acta Mechanica Sinica, Vol. 18, pp. 594-602.
24. Lien F. S. and Leschziner M. A., (1994). *"Assessment of turbulent transport models including nonlinear RNG eddy-viscosity f*ormulation and second-moment closure", Computers and Fluids, Vol. 23, No. 8, pp. 983-1004.
25. Wilcox D. C., (1993). "*Turbulence Modeling for CFD*", DCW Industries Inc., La Canada, California.
26. Launder B. and Spalding B. D., (1974). "*The Numerical Computation of Turbulent Flows*", Computer Methods in Applied Mechanics and Engineering, No. 3.
27. Choudhury D., (1993). "*Introduction to the Renormalization Group Method and Turbulence Modeling*", Fluent Inc. Technical Memorandum TM-107.
28. Shih T. H., Liou W., Shabbir A., and Zhu J., (1995). "*A New k-ε Eddy-Viscosity Model for High Reynolds Number Turbulent Flows - Model Development and Validation*", Computers Fluids, Vol. 24, No. 3, pp. 227-238.
29. Hirt C. W. and Nichols B. D., (1981). "*Volume of fluid (VOF) method for the dynamics of free boundaries*", Journal of Computational Physics, Vol. 39, No. 1, pp. 201-225.